Proc. Natl. Acad. Sci. USA
Vol. 94, pp. 4389–4394, April 1997
Biophysics

Charge separation in the reaction center of photosystem II studied as a function of temperature

(electron transfer/energy transfer/photosynthesis)

MARIE-LOUISE GROOT†, FRANK VAN MOURIK, CAMIEL EIJCKELHOFF, IVO H. M. VAN STOKKUM, JAN P. DEKKER, AND RIENK VAN GRONDELLE

Department of Physics and Astronomy and Institute of Molecular Biological Sciences, Vrije Universiteit, De Boelelaan 1081, 1081 HV Amsterdam, The Netherlands

Communicated by George Porter, Imperial College of Science, Technology, and Medicine, London, United Kingdom, January 13, 1997 (received for review April 30, 1996)

ABSTRACT **In photosystem II of green plants the key photosynthetic reaction consists of the transfer of an electron from the primary donor called P680 to a nearby pheophytin molecule. We analyzed the temperature dependence of this reaction by subpicosecond transient absorption spectroscopy over the temperature range 20–240 K using isolated photosystem II reaction centers from spinach. After excitation in the red edge of the Q_y absorption band, the decay of the excited state can conveniently be described by two kinetic components that both accelerate with temperature. This temperature behavior differs remarkably from that observed in purple bacterial reaction centers. We attribute the first component, which accelerates from 2.6 ps at 20 K to 0.4 ps at 240 K, to charge separation after direct excitation of P680, and explain its temperature dependence by an intermediate that lies in energy above the singlet-excited P680 and that possibly has charge-transfer character. The second component accelerates from 120 ps at 20 K to 18 ps at 240 K and is attributed to charge separation after direct excitation of the "trap" state near-degenerate with P680 and subsequent slow energy transfer from this trap state to P680. We suggest that the slow energy transfer from the trap state to P680 plays an important role in the kinetics of radical pair formation at room temperature.**

The photochemical reaction center (RC) of photosystem II (PSII) (the D1–D2 cyt.*b*559 complex) is the smallest unit in PSII that shows photochemical activity. The RC contains six chlorophyll (Chl) *a* and two pheophytin (Pheo) *a* molecules (1–4) that all have their lowest electronic transition around 675 nm, as well as two β-carotenes. The D1 and D2 polypeptides are homologous to the L and M subunits of bacterial RCs, suggesting an arrangement of the core pigments in the RC of PSII similar to that in the bacterial RC (5). The two additional Chl molecules are probably located near the periphery of the D1–D2 complex.

The characterization of energy transfer and charge separation in the PSII RC is less well established than is the case for the bacterial RC (for a review, see ref. 6). This may be due to the fact that the first PSII RC was isolated only in 1987 (7) and that there is no structure available. However, the excited state kinetics of the PSII RC are also inherently more complicated than those of bacterial RCs. The primary electron donor in PSII, called P680, is isoenergetic with some of the other pigments in the RC (8–13) and as a consequence forms only a very shallow trap for excitations.

After excitation of P680 an electron is transferred to the photoactive Pheo molecule (6). In isolated PSII RC preparations, further electron transport cannot occur, because the quinone acceptors are lost during the isolation procedure. A straightforward interpretation of the results from pump–probe measurements in terms of pigment to pigment energy transfer and charge separation rates has proven difficult, mainly due to the congested absorption spectrum of the PSII RC. At room temperature (RT), most groups observed kinetics with lifetimes of 1–3 ps, 10–20 ps and >1 ns (14–20) as well as 100–600 fs (21–27). At very low temperature (4 K) the lifetime of singlet-excited P680 (P680*) was estimated to be 1.9 ps by transient hole-burning spectroscopy (28). Based on this result and on the work in ref. 29, it was suggested that the rate of primary charge separation increases upon lowering the temperature, similar to what has been observed for the rate of charge separation in the purple bacterial RC (30). However, it is not clear whether or not the 1.9-ps time constant at 1.4 K and the 3- or 20-ps processes at RT can be attributed to the same physical process. Furthermore, most recent studies (19, 20, 22, 27, 31) conclude that radical pair formation in the PSII RC is too complicated to assign one kinetic component to charge separation.

Low temperature subpicosecond measurements are a valuable method to obtain more information on the primary processes since, due to slowing down of uphill energy transfer, the kinetics can be related to one of the primary processes in a more straightforward manner. The particular temperature dependence of the kinetics will yield information on their origin. We have performed transient absorption measurements between 20 K and 240 K employing selective (≈5 nm spectral width) excitation of the most red-absorbing P680 and "trap" pigments (9, 13). Our results show that at low temperature the excited state decay of the PSII RC due to radical pair formation gives rise to two kinetic components that both accelerate with increasing temperature, in contrast to charge separation in bacterial RCs.

MATERIALS AND METHODS

PSII RC (D1–D2 cyt.*b*559) complexes were isolated from spinach by means of a short Triton X-100 treatment of CP47–RC complexes as described (4), but with the modification that a high, 1% concentration of dodecyl maltoside was added to the RCs immediately after Triton X-100 incubation and before loading on the anion exchange column. The samples were characterized by a ratio of the RT absorptions at

The publication costs of this article were defrayed in part by page charge payment. This article must therefore be hereby marked "*advertisement*" in accordance with 18 U.S.C. §1734 solely to indicate this fact.

0027-8424/97/944389-6$2.00/0
PNAS is available online at **http://www.pnas.org**.

Abbreviations: PSII, photosystem II; RC, reaction center; P680, primary electron donor of PSII; DAS, decay-associated spectrum; RT, room temperature; FWHM, full width at half maximum; Chl, chlorophyll; Pheo, pheophytin; CT, charge transfer.

†To whom reprint requests should be addressed.

416 nm and 435 nm of 1.20 and contained, according to the method reported in ref. 4, Chl *a*, Pheo *a*, and β-carotene in a ratio of 6.5:2.0:2.0. The samples were diluted in a buffer containing 20 mM BisTris (pH 6.5), 20 mM NaCl, 0.03% *n*-dodecyl-β-D-maltoside, and 80% (vol/vol) glycerol to an optical density of ≈1.0 at 675 nm in a cuvette with 1.5 mm path length. The samples were placed in either a nitrogen bath cryostat or a helium flow cryostat. The laser system has been described in detail elsewhere (31, 32), it was modified by using sapphire plates for the creation of the white light continuum, and the use of a single dye cell for the amplification of the pump beam. The system had an instrument response full width at half maximum (FWHM; cross correlation of pump and probe pulse) of 250–280 fs, from which we estimate the pump pulse to be ≈180 fs. The excitation energy of the pump beam was about 250 nJ/pulse, focused with a 20-cm lens to a spot size in the sample of ≈275 μm in diameter. Excitation was at ≈685 nm, using a narrow-band (5 nm FWHM) interference filter. The probe beam was polarized under magic angle (54.7°) with the pump. The repetition rate of the system was 30 Hz, therefore no accumulation of RCs in the triplet state could occur (9). Because of the slight divergence of the laser pump beam (which went through a variable delay and therefore varied in diameter as a function of the delay) we placed an aperture in the pump beam just before the focusing lens to maintain a fixed size of the focus, leading to a variation in the pump energy of up to 20% for long delays. Spectra were corrected for the energy of the pump beam at the position of the sample, which was measured as a function of the delay line. Usually 6 scans, consisting of 40 delay positions, were taken for data collection. In a single scan, about 300 shots were averaged per delay position, both with and without excitation light on the sample. We analyzed the data with the help of singular value decomposition (33). From the number of singular values and vectors significantly different from the noise, we determined the number of spectrally and temporally independent components. Decay-associated spectra (DAS) were estimated from a global analysis procedure (33), performed on all individual scans simultaneously, in which the data were described with a model of parallelly decaying compartments: $\Delta A(\lambda,t) = \Sigma_i\ \Delta OD_i(\lambda)\exp(-t/\tau_i) * i(t)$, where $i(t)$ is the instrument response and * denotes convolution. The instrument response was described in the global analysis by a Gaussian shape. The location and width of the instrument response were fit parameters for each scan. All fits had a standard deviation of the residuals between 1.3% and 2.8% of the maximal bleaching.

We checked that the induced ΔOD signals responded linearly to a variation in the excitation density. Furthermore, from the induced ΔOD signals, using the method described in (34), we estimated that after 150 ps 12–16% of the RC is in the radical pair state. (See ref. 34 for further discussion.)

RESULTS

Absorbance difference spectra induced by 180 fs laser flashes centered at 685 nm (FWHM, 5 nm) were recorded as a function of time delay at five temperatures: 20, 77, 110, 150, and 240 K. Fig. 1 shows some of the spectra taken at 20 K at time delays between 0.4 ps and 750 ps. Note that we define t = 0 as the last time point before a ΔOD signal occurs. The first few spectra (data not shown) within the in-growth of the signal, are characterized by a narrow bleaching (FWHM ≈ 4–5 nm) centered at 682.5 nm, and a positive signal between 673 and 680 nm. After ≈250 fs the bleached spectrum has shifted to 683 nm and has a structureless absorption increase at wavelengths shorter than 678 nm. The maximal bleaching occurs after 0.5 ps. At later times, the intensity of the signal near 683 nm diminishes, while at 675 nm a second bleach develops as a shoulder on the major peak at 683 nm. The absorption increase

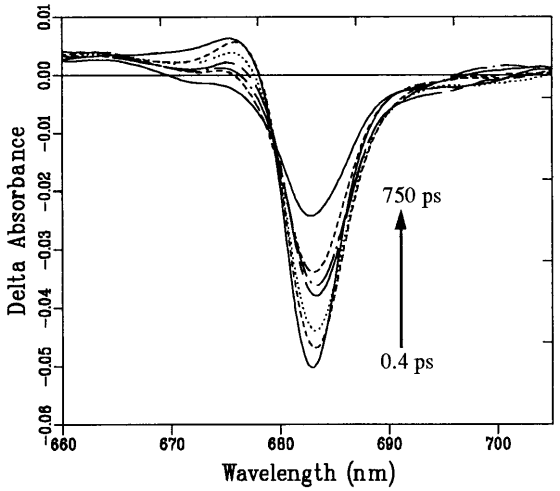

FIG. 1. Temperature = 20 K, λ_{exc} = 685 nm. ΔOD spectra at time delays of 0.4 ps (solid line), 1.0 ps (dashed line), 4.75 ps (dotted line), 21 ps (chain-dash line), 55 ps (chain-dotted line), 155 ps (dashed line), and 750 ps (solid line)

between 660 nm and 670 nm remains constant over the same time window. The last spectrum, taken at 750 ps, has a FWHM of 7 nm and represents, at least for the major part, the radical pair spectrum.

The spectra recorded at higher temperatures (data not shown) are broader and less structured and reveal different time constants, but otherwise show essentially the same characteristics. The radical pair spectra taken at 750 ps show a well-defined shoulder up to 110 K. Above this temperature the shoulder is diminished, which is probably due to thermal broadening. At 240 K, the FWHM of the spectrum at 750 ps is 10 nm.

Satisfactory fits of the data sets could be obtained at all temperatures using three kinetic components, as well as a component that instantaneously follows the excitation pulse. At 20 K, the first component has a lifetime of 2.6 ps, and is characterized by a DAS with a minimum at 682.5 nm, a FWHM of 4.5 nm and an absorption increase at wavelengths shorter than 679 nm (dotted line in Fig. 2). The second component

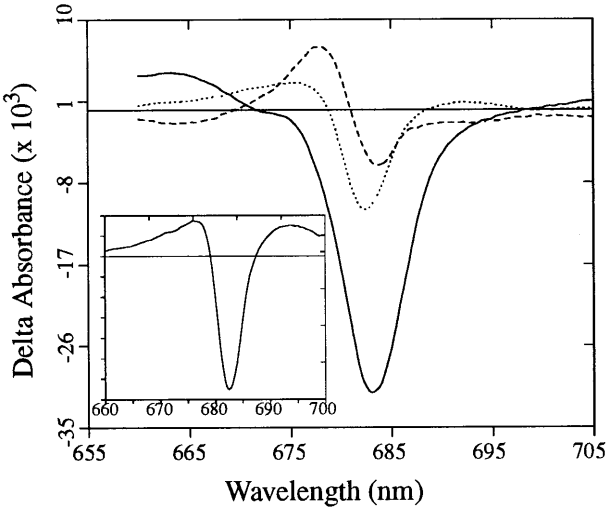

FIG. 2. DAS at T = 20 K of the 2.6-ps (dotted line), 120-ps (dashed line), and 2-ns (solid line) components. (*Inset*) DAS spectrum of the component that follows the excitation pulse instantaneously and which is responsible for a ΔOD of 14.10^{-3} at the maximum of the instrument response. At all temperatures such a component was included in the fit.

(dashed line in Fig. 2) has a lifetime of 120 ps and its DAS is characterized by a maximum at 678 nm, a zero crossing at 681 nm and a minimum at 683.5 nm. The third spectrum (solid line) is almost nondecaying; in the fit its lifetime is estimated to be 2 ns. It has a minimum at 683 nm, a FWHM of 7 nm and shows a small negative shoulder around 672.5 nm.

Fig. 2 *Inset* shows the DAS of the component t0 that follows the excitation pulse instantaneously—i.e., is only observed in the presence of the excitation pulse. For comparison (although we do not have the time resolution to resolve this component), when the data were fitted with an additional fast component instead of one that follows directly the excitation pulse, a lifetime of ≈40–80 fs was obtained. At all temperatures such a fast feature with similar shape and amplitude was present in the data. This ultrafast spectral feature most likely arises from the intrinsic intensity dependence of a polarized pump–probe experiment, in which the center of the ΔOD spectrum saturates even at relatively low excitation density (ref. 34; M.-L.G., R.V.G., J. A. Leegwater, and F.v.M., unpublished data). As a consequence the ΔOD spectrum broadens during the excitation pulse, in agreement with the DAS of the fast component.

Each of the fits at 77 K, 110 K, 150 K, and 240 K yields a DAS of the first component that shows a loss of oscillator strength in the red part of the spectrum and a minor absorption increase in the blue (see Fig. 3, dotted lines), similar to that of the first component at 20 K. With increasing temperature, the magnitude of this component increases relative to that of the other two. The time constant related to these absorption changes decreases from 2.6 ps at 20 K to about 0.5 ps at 240 K (see Table 1). The DAS that are found for the second components are all nearly conservative, except for the one at 240 K which contains no positive feature (Fig. 3, dashed lines). The lifetime of this component decreases from 120 ps at 20 K to 18 ps at 240 K (Table 1).

The lifetimes from our fit at 240 K differ somewhat from those reported at RT, where the initial decay is described by lifetimes of 100–250 fs, ≈1–3 ps and 15–20 ps (20–27), in which the amplitude of the 1- to 3-ps component is usually small relative to the other components. First of all we note that in a complex system like PSII when one process is not fitted correctly, other components will easily be influenced as well. From our singular value decomposition we conclude that the four components are kinetically and spectrally independent. Furthermore, the magnitude and rate of τ_0 is independent of temperature, which indicates that it is not in any way mixed with an energy transfer component, since this would result in a dramatic temperature dependence of the amplitude of the τ_0 component. Possibly, in fitting RT results the τ_0 component has been mixed with a true energy transfer component and compensation of the remaining spectral and kinetic features led to the 1- to 3-ps component.

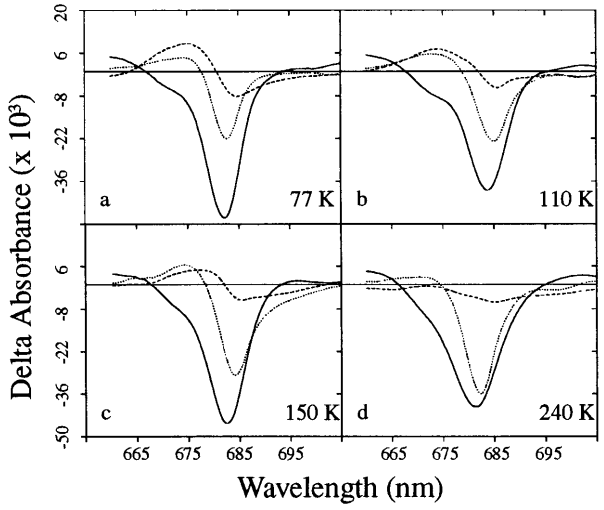

FIG. 3. DAS if T = 77 K, 0.7 ps (dotted line), 34 ps (dashed line) (*a*), T = 110 K, 0.5 ps (dotted line), 37 ps (dashed line) (*b*), T = 150 K, 0.5 ps (dotted line), 33 ps (dashed line) (*c*), and T = 240 K, 0.4 ps (dotted line), 18 ps (dashed line) (*d*). The long-lived spectra are indicated by the solid lines.

Table 1. Results of the global analyses of the data sets recorded at 20, 77, 110, 150, and 240 K

T	20 K	77 K	110 K	150 K	240 K
τ_1, ps	2.6	0.7	0.5	0.5	0.4
τ_2, ps	120	34	37	33	18
τ_3, ns	2	4	9	∞	6

In the fits a component that follows the pump pulse instantaneously (τ_0) was included at all temperatures. The error in the lifetimes is about 10%, except for τ_3, of which the lifetime cannot be determined well in this experiment.

DISCUSSION

In this work we have studied the excited state and charge separation dynamics of the PSII RC as a function of temperature between 20 K and 240 K. Red excitation ($\lambda_{exc} < 685$ nm) was applied to avoid the involvement of the peripheral Chls absorbing around 670 nm. Our results demonstrate that at all temperatures a major part of the excited state dynamics of the PSII RC upon red excitation is determined by a fast and a slower decaying component, each with its own DAS. Both components accelerate with temperature, which is in contrast to the situation in the bacterial RC where the rate associated with radical pair formation decreases with temperature (30).

Radical Pair Spectrum. The long-lived component is readily assigned to be mainly due to the radical pair state $P680^+Pheo$. This state has been reported to have a lifetime of tens of nanoseconds at low temperature (35, 36), and its spectrum at 240 K is very similar to that reported earlier at RT by Klug *et al.* (ref. 22 and references therein). At low temperatures the shoulder around 670–675 nm is well separated from the main bleaching at 682–683 nm.

The 120 → 18-ps Component. This component shows at all temperatures, except at 240 K, a DAS that corresponds to a loss of oscillator strength on the red side of the spectrum and an increase of about the same magnitude on the blue side (dashed lines in Figs. 2 and 3). Although at first sight this might represent a typical energy transfer process from red to blue absorbing states, this cannot be the case. At low temperature the thermal energy (14 cm^{-1} at 20 K) is too small to result in a significant population of states that are ≈120 cm^{-1} higher in energy. Therefore this spectral change around 675 nm must be related to the decay of excited state absorption of the initial state and the formation of the radical pair bleaching around 675 nm.

Upon excitation at 685 nm only the most red-absorbing states are excited (see, for example, the energy level diagram in Fig. 4). We have shown (9, 13, 31) that in this wavelength region besides P680 the so-called trap state absorbs as well. These pigments are not part of the primary donor and can actually trap excitations at low temperature. At $T < 4$ K these pigments have been shown to have excited state lifetimes of either about 200 ps or 4 ns depending on whether or not they are able to transfer energy (13), which is determined by their position within the inhomogeneously broadened bands. At 20 K the excited state lifetime of the trap is expected to be shorter, since the activation energy between the trap and P680 levels is probably very small, about 1 or 2 nm (9, 13). The attribution of the 120-ps lifetime to the excited state lifetime of the trap is therefore in good agreement with the hole-burning results. We thus conclude, from its spectral changes and its lifetime,

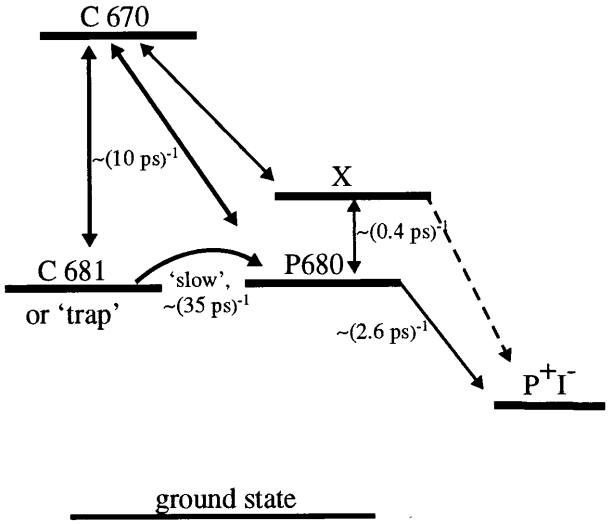

FIG. 4. Energy level diagram of the states of the PSII RC involved in energy transfer and charge separation. C670, C681, and P680 denote (groups of) pigments or states absorbing at that particular wavelength; arrows denote energy transfer and charge separation. All reactions are reversible, but those that are on the time domain of interest effectively unidirectional are indicated as such. Note that due to inhomogeneous broadening the energy levels are actually broader as depicted here (≈5 nm FWHM) and therefore overlap extensively. C670 represents one or two pigments that transfer slowly [≈15 ps (13, 31, 37)] to the other pigments and can be inferred at $T \geq 240$ K to equilibrate with the states absorbing around 680 nm in about 10 ps; C681 or the trap-state is degenerate with P680 and transfers to P680 directly in ≈35 ps or slower at low temperature; P680 is the primary electron donor; and X may represent the higher excitonic multimer levels or a multimer state with charge transfer character that mediates electron transfer from P680*. The 2.4 → 0.4-ps component is essentially ascribed to equilibration between P680 and X and its decay into P^+I^-, the 120 → 18-ps component to the C681 to P680 transfer which at higher temperature is accelerated through the C681 → C670 → P680 decay channel (see *Discussion*).

that the 120-ps component can be assigned to effective radical pair formation upon direct trap excitation, limited by slow energy transfer from the trap pigments to P680 (Fig. 4).

At higher temperatures, between 77 K and 150 K, the lifetime of the 120 → 18-ps component has decreased to a value of about 35 ps (see Table 1 and dashed lines in Fig. 3), which shows that the activation energy at this temperature is much smaller than the thermal energy (to get an indication of the activation energy, the temperature dependence of this component between 20 K and 150 K corresponds with an activation energy of 19 cm^{-1} or 1 nm). This is in agreement with the assignment of this component to energy transfer between the near-degenerate trap and P680 states.

At 240 K, the lifetime of this component has decreased to 18 ps, close to the 21-ps time constant reported to be responsible for the major part of radical pair formation at RT (22). A probable explanation for this acceleration is that at this temperature the trap pigments equilibrate with the blue (≈670 nm) absorbing pigments prior to the decay of the excited state into the radical pair. These pigments are often speculated to be the two "extra" Chls, presumably located at some distance from the "core" pigments. At 240 K the mixture of this equilibration process with the decay of the equilibrated state into the radical pair state is probably the reason why the DAS of the second component no longer exhibits the positive signal; the contributions of the equilibration component (which is expected to show a negative signal in the red and a positive signal in the blue part of the spectrum) and the decay of the equilibrium due to radical pair formation (which should be accompanied by a loss of oscillator strength in the more blue part of the spectrum) overlap and partly cancel each other. Müller *et al.* (27) probably resolved these components at 277 K; the DAS spectra of their 8.9-ps and 19.8-ps components observed upon 680 nm excitation resemble those inferred above for the equilibration process and the decay of the equilibrium, respectively. We suggest that at RT at least part of radical pair formation occurring with a ≈20-ps time constant (ref. 22 and references therein) is limited by energy transfer from the trap pigments near-degenerate with P680, and by equilibration of the trap state with "blue" absorbing states before excitation energy transfer to P680 takes place.

In Visser *et al.* (31) we reported a lifetime of 80–100 ps at 77 K for the 120 → 18-ps component. The difference in lifetime with the 77 K value reported here is probably due to a slight variation in the samples that were used. The PSII RC preparations used in the experiments reported here were obtained following a more gentle isolation procedure, as described in *Materials and Methods*. They are characterized by a deeper valley between the main bands in the 4 K absorption spectrum, and by a more pronounced shoulder at 684 nm than observed for the preparations used in the earlier experiments (31). In Eijckelhoff *et al.* (38) this subtle change in the Q_y region is explained by a narrowing of the underlying absorption bands in the red part of the spectrum, from ≈6 nm to ≈4 nm. A narrowing of the inhomogeneous absorption bands of both P680 and the trap pigments will lead to a decrease in the average activation energy between the trap pigments and P680. Therefore, the onset of acceleration of the average energy transfer time as a function of temperature may be expected to occur at lower temperature. To explain the acceleration from 90 ps to 35 ps, assuming an Arrhenius type of expression, at 77 K a change in activation energy of only 49 cm^{-1} or 2.2 nm is needed, which is consistent with the observed narrowing (38). Although the variation of the samples is discomforting, it lends support for the notion that the observed temperature behavior of the kinetics originates from the inhomogeneity of two degenerate electronic transitions.

The Nature of the Trap State. Our experiments have shown that in the PSII RC a trap state exists near-degenerate with P680 (9, 13), that at temperatures below 150 K, but possibly also at higher temperatures, is involved in slow radical pair formation. We estimate that upon red excitation about 50% of the excitations drive charge separation along a path involving the trap state, while the remaining excitations directly excite P680. We can only speculate about the nature of the trap state. Fluorescence experiments (11) have demonstrated the contribution of Chl *a* and possibly Pheo *a* in the low temperature emission spectrum, which originates from the trap state. Hole-burning experiments have also indicated the presence of Pheo *a* (8, 13). To explain a variety of spectroscopic and kinetic observations it has been proposed (39) that in the PSII RC all excitonic coupling strengths are of similar magnitude and also similar to the amount of disorder (≈100 cm^{-1}). The result of this multimer model is that for each RC there are two strongly allowed states, on average one is localized on the pigments in the active branch and the second on the inactive branch. The precise energetic ordering and composition of these two states varies due to the disorder, both states contain Chl *a* and Pheo *a*. If we assume that only the state localized on the active branch drives ultrafast electron transfer, then at $T < 4$ K the "inactive" state will act as a trap in those RCs in which this state is lower in energy than the active state. At higher temperatures the inactive exciton state can relax into the "active" state and drive charge separation in all centers. Our experiments suggest that even at RT this direct relaxation process is not ultrafast and possibly takes up to tens of picoseconds. This would imply that the coupling between the pigments in the active state with those in the inactive state is relatively weak. We note that in the even more tightly packed light-harvesting complex II of green plants some of the energy

transfer between the Chl *a* molecules in the same subunit may take as long as 10 ps due to an unfavorable orientation of some of the pigments (40).

The 2.6 → 0.4-ps Component. The basic feature of the DAS of the 2.6 → 0.4-ps component (dotted lines in Figs. 2 and 3) is a loss of bleaching on the red side of the spectrum and a relatively weak in-growth (or loss of excited state absorption) below 678 nm at all temperatures. It is tempting to attribute this fast component to charge separation upon direct P680 excitation at all temperatures, at 20 K this is the only reasonable explanation for the observed decay. Note that this time constant is somewhat slower than that observed for the bacterial RC [1.4 ps for *Rhodobacter sphaeroides*, 0.9 ps for *Rhodopseudomonas viridis* (30) vs. 2.6 ps for PSII RC].

The attribution of the 2.6 → 0.4-ps component to direct charge separation means, however, that the charge separation accelerates with temperature, in contrast to earlier suggestions that the charge separation time in the PSII RC decreases with temperature, to 1.2 ps at 15 K (29) or 1.9 ps at 4 K (28). These suggestions were, however, based on the assumption that the 1- to 2-ps kinetics could be identified with a 3-ps component observed in RT measurements. Our results indicate that the decay of P680* is due to an activated processes, unlike in the bacterial RC, and that the (nonactivated) intrinsic charge separation time is 300–400 fs at RT, which is much faster than in the bacterial system. Two other groups have reported on subpicosecond processes at RT, but did not relate these to charge separation processes: the London group ascribed a 100-fs time constant to equilibration between red and blue states of the (multimer) core of pigments (21, 22) and a 500-fs time constant, which was mainly observed as a decay of the anisotropy, to energy transfer between two near-degenerate red states (41). Holzwarth and coworkers (27) mentioned the existence of a 250-fs time constant in their data and ascribed it to equilibration within a core of RC pigments. As with Müller *et al.* (27), we have not observed a 100-fs time constant, although we did observe a very fast (40–80 fs) component. But as discussed above, we do not ascribe this component to one of the physically relevant primary processes in PSII, especially since in our experiments this component is not influenced by temperature. The amplitude of an uphill equilibration process would be very temperature-dependent, and therefore the fast (40–80 fs) component is not consistent with energy transfer. Our results show that the 400-fs component, which most likely can be identified with the 250 fs and 500 fs of refs. 27 and 41, extrapolates to a low temperature value of 2.6 ps. This temperature dependence is in fact rather weak and corresponds to an activation energy of only ≈1.5–2 nm. This suggests that the decay of P680* is not due to energy transfer to blue (≈670–675 nm) states, but rather to a near-degenerate state, in agreement with the suggestion in Merry *et al.* (41). This state can, however, not be the trap state, as was suggested in in ref. 41, since the results discussed in the previous section show that the trap-to-P680 transfer is much slower than 2.6–0.4 ps. Furthermore, the spectral changes associated with the 2.6 → 0.4-ps time constant are rather large and this suggests that a transition occurs to a state of low oscillator strength, or dark state, whereas the trap state has a more or less comparable oscillator strength to that of P680 (9, 13). According to the multimer model, the multimer states of low-oscillator strength are in the ≈670–675 nm region, too high in energy to be in accordance with the temperature dependence of the 2.6 → 0.4-ps component.‡ In the following, we will discuss the possibility that at all temperatures the 2.6 → 0.4-ps component is due to direct charge separation and how the multimer nature of P680 could be the cause of its peculiar temperature dependence.

‡Of course we cannot exclude the possibility that one of multimer states is actually lower in energy and thus equilibration within the exciton manifold of the multimer is the origin of this component.

The multimer model (39) implies that P680 consists of a multimer of weakly coupled pigments, including the Pheo acceptor. For this reason it is of interest to compare the PSII RC to the heterodimer mutants M200 and L173 of *Rhodobacter capsulatus* and *Rb. sphaeroides*, where one of the bacteriochlorophylls of the special pair has been replaced by a bacteriopheophytin. In these mutants an intradimer charge transfer occurs, the energy of the intradimer charge transfer state is most likely near the excitonic state of the heterodimer (42–45). Recently, the formation of a change transfer (CT) state in 200 fs was also proposed to occur in the wild-type bacterial RC (46). As in the heterodimer, the involvement of the Pheo acceptor in the multimer probably leads to less electronic symmetry in PSII as compared with the primary donor in bacterial RCs, and so charge transfer states may be expected to play a role in the excited multimer states. Therefore it may be that the 2.6 → 0.4-ps kinetics correspond to the evolution of the initially excited P680 state to a state with more charge transfer character, from which the charge separated state is formed (state X and the dashed arrow in Fig. 4). The formation of the CT state (or rather the formation of an equilibrium between the initially excited state and the CT state) will be accompanied by a loss of stimulated emission in the red part and of excited state absorption in the blue part of the spectrum, in agreement with the spectral changes of the 2.6 → 0.4-ps component. Note that as far as we can see, neither the hypothesis of the formation of a CT state, nor equilibration within the exciton manifold (of which the spectrum of the equilibrated multimer state would have to be similar to the $P680^+I^-$ state to explain the absence of subsequent spectral changes related to radical pair formation) explain why the amplitude of the 2.6 → 0.4-ps component increases with temperature relative to that of the radical pair spectrum. Possibly changes in the excited spectral distribution due to the temperature dependence of the absorption spectra, or even a slight modification of the nature of the multimer with temperature might be the cause for this.

Though the involvement of a CT state would suggest that the actual charge separation process may be looked upon as an adiabatic electron transfer process, it remains possible that direct (nonadiabatic) charge separation occurs from the initially excited P680, but on a slower time scale. An upper limit for the intrinsic charge separation rate from P680 would then be the rate constant at 20 K so $\approx(2.6\ \text{ps})^{-1}$.

Fig. 4 provides a summary of the results obtained in this paper and in previous work (9, 13, 31) in the form of a model for the energetics and kinetics of the PSII RC.

CONCLUSIONS

The temperature dependence of the excited state decay of PSII RCs as measured by subpicosecond transient absorption spectroscopy is different from that of bacterial RCs, reflecting the complex electronic level structure of this plant RC. A fast process, that accelerates from 2.6 ps at 20 K to 0.4 ps at 240 K, is associated with direct charge separation involving P680—i.e., an electronic state in the multimer model (14) mainly localized on the active branch. A much slower process that accelerates from 120 ps at 20 K to 18 ps at 240 K is associated with slow energy transfer from the trap state (9, 13)—i.e., the electronic state in the multimer localized on the inactive branch. It is argued that even at temperatures close to RT, the equilibration between these two states is relatively slow, possibly due to some unfavorable geometry and as a consequence part of radical pair formation is energy transfer limited.

We are grateful to Henny van Roon for the expert preparation of the PSII RC particles and to Matthieu Visser for his efforts with the laser system. The research was supported by European Community Contract CT940619 and by the Netherlands Organization for Scientific

Research via the Dutch Foundations for Physical and Chemical Research and for Life Sciences.

1. Kobayashi, M., Maeda, H., Watanabe, T., Nakane, H. & Satoh, K. (1990) *FEBS Lett.* **260,** 138–140.
2. Gounaris, K., Chapman, D. J., Booth, P., Crystall, B., Giorgi, L. B., Klug, D. R., Porter, G. & Barber, J. (1990) *FEBS Lett.* **265,** 88–92.
3. van Leeuwen, P. J., Nieveen, M. C., van de Meent, E. J., Dekker, J. P. & van Gorkom, H. J. (1991) *Photosynth. Res.* **28,** 149–153.
4. Eijckelhoff, C. & Dekker, J. P. (1995) *Biochim. Biophys. Acta* **1231,** 21–28.
5. Michel, H. & Deisenhofer, J. (1988) *Biochemistry* **27,** 1–7.
6. van Grondelle, R., Dekker, J. P., Gillbro, T., Sundström, V. (1994) *Biochim. Biophys Acta* **1187,** 1–65.
7. Nanba, O. & Satoh, K. (1987) *Proc. Natl. Acad. Sci. USA* **84,** 109–112.
8. Tang, D., Jankowiak, R., Seibert, M., Yocum, C. F. & Small, G. J. (1990) *J. Phys. Chem.* **94,** 6519–6522.
9. Groot, M.-L., Peterman, E. J. G., van Kan, P. J. M., van Stokkum, I. H. M., Dekker, J. P. & van Grondelle, R. (1994) *Biophys. J.* **67,** 318–330.
10. Chang, H.-C., Small, G. J. & Jankowiak, R. (1994) *Chem. Phys.* **194,** 323–333.
11. Kwa, S. L. S., Tilly, N. T., Eijckelhoff, C., van Grondelle, R. & Dekker, J. P. (1994) *J. Phys. Chem.* **98,** 7712–7718.
12. Konermann, L. & Holzwarth, A. R. (1996) *Biochemistry* **35,** 829–842.
13. Groot, M.-L., Dekker, J. P., van Grondelle, R., den Hartog, F. T. & Völker, S. (1996) *J. Phys. Chem.* **100,** 11488–11495.
14. Wasielewski, M. R., Johnson, D. G., Seibert, M. & Govindjee (1989) *Proc. Natl. Acad. Sci. USA* **88,** 524–528.
15. Roelofs, T. A., Gilbert, M., Shuvalov, V. A. & Holzwarth, A. R. (1991) *Biochim. Biophys. Acta* **1060,** 237–244.
16. Gatzen, G., Griebenow, K., Müller, M. G. & Holzwarth, A. R. (1992) in *Research in Photosynthesis*, ed. Murata, N. (Kluwer, Dordrecht, The Netherlands), Vol. 2, pp. 69–72.
17. Schelvis, J. P. M., van Noort, P. I., Aartsma, T. J. & van Gorkom, H. J. (1994) *Biochim. Biophys. Acta* **1184,** 242–250.
18. Wiederrecht, G. P., Seibert, M., Govindjee & Wasielewski, M. R. (1994) *Proc. Natl. Acad. Sci. USA* **91,** 8999–9003.
19. Donovan, B., Walker, L. A., Yocum, C. F. & Sension, R. J. (1996) *J. Phys. Chem.* **100,** 1945–1949.
20. Greenfield, S. R., Seibert, M., Govindjee & Wasielewski, M. R. (1996) *Chem. Phys.* **210,** 279–295.
21. Durrant, J. R., Hastings, G., Joseph, D. M., Barber, J., Porter, G. & Klug, D. R. (1992) *Proc. Natl. Acad. Sci. USA* **89,** 11632–11636.
22. Klug, D. R., Rech, Th., Joseph, D. M., Barber, J., Durrant, J. R. & Porter, G. (1995) *Chem. Phys.* **194,** 433–442.
23. Rech, Th., Durrant, J., Joseph, D. M., Barber, J., Porter, G. & Klug, D. R. (1994) *Biochemistry* **33,** 14768–14774.
24. Hastings, G., Durrant, J. R., Barber, J., Porter, G. & Klug, D. R. (1992) *Biochemistry* **31,** 7638–7647.
25. Durrant, J. R., Hastings, G., Joseph, D. M., Barber, J., Porter, G. & Klug, D. R. (1993) *Biochemistry* **32,** 8259–8267.
26. Holzwarth, A. R., Müller, M. G., Gatzen, G., Hucke, M. & Griebenow, K. (1994) *J. Lumin.* **60,** 497–502.
27. Müller, M. G., Hucke, M., Reus, M. & Holzwarth, A. R. (1996) *J. Phys. Chem.* **100,** 9527–9536.
28. Jankowiak, R., Tang, D., Small, G. J. & Seibert, M. (1989) *J. Phys. Chem.* **93,** 1649–1654.
29. Wasielewski, M. R., Johnson, D. G., Govindjee, Preston, C. & Seibert, M. (1989) *Photosynth. Res.* **22,** 89–99.
30. Fleming, G. R., Martin, J. L. & Breton, J. (1988) *Nature (London)* **333,** 190–195.
31. Visser, H. M, Groot, M.-L., van Mourik, F., van Stokkum, I. H. M., Dekker, J. P. & van Grondelle, R. (1995) *J. Phys. Chem.* **99,** 15304–15309.
32. Visser, H. M., Somsen, O. J. G., van Mourik, F., Lin, S., van Stokkum, I. H. M. & van Grondelle, R. (1995) *Biophys. J* **69,** 1083–1099.
33. van Stokkum, I. H. M., Scherer, T., Brouwer, A. M. & Verhoeven, J. W. (1994) *J. Phys. Chem.* **98,** 852–866.
34. Groot, M.-L. (1997) Ph.D. thesis (Free Univ. of Amsterdam, Amsterdam), pp. 1–139.
35. van Kan, P. J. M., Otte, S. C. M., Kleinherenbrink, F. A. M., Nieveen, M. C., Aartsma, T. J. & van Gorkom, H. J. (1990) *Biochim. Biophys. Acta* **1020,** 146–152.
36. Volk, M., Gilbert, M., Rousseau, G., Richter, M., Ogrodnik, A. & Michel-Beyerle, M.-E. (1993) *FEBS Lett.* **336,** 357–362.
37. Roelofs, T. A., Kwa, S. L. S., van Grondelle, R., Dekker, J. P. & Holzwarth, A. R. (1993) *Biochim. Biophys. Acta* **1143,** 147–157.
38. Eijckelhoff, C., van Roon, H., Groot, M.-L., van Grondelle, R. & Dekker, J. P. (1996) *Biochemistry* **35,** 12864–12872.
39. Durrant, J. R., Klug, D. R., Kwa, S. L. S., van Grondelle, R., Porter, G. & Dekker, J. P. (1995) *Proc. Natl. Acad. Sci. USA* **92,** 4798–4802.
40. Visser, H. M., Kleima, F., van Grondelle, R., van Amerongen, H. (1996) *Chem. Phys.* **210,** 297–312.
41. Merry, S. A. P., Kumazaki, S., Tachibana, Y., Joseph, D. M., Porter, G., Yoshihara, K., Barber, J., Durrant, J. R. & Klug, D. R. (1996) *J. Phys. Chem.* **100,** 10469–10478.
42. Takahashi, E. & Wraight, C. A. (1994) *Adv. Mol. Cell Biol.* **10,** 197–251.
43. Kirmaier, C., Bylina, E. J., Youvan, D. C. & Holten, D. (1989) *Chem. Phys. Lett.* **159,** 251–257.
44. McDowell, L. M., Kirmaier, C. & Holten, D. (1990) *Biochim. Biophys. Acta* **1020,** 239–246.
45. McDowell, L. M., Kirmaier, C. & Holten, D. (1991) *J. Phys. Chem.* **95,** 3379–3383.
46. Hamm, P. & Zinth, W. (1995) *J. Phys. Chem.* **99,** 13537–13544.